Improved Wheeler Cap Method Based on an Equivalent High-Order Circuit Model

Chihyun Cho, *Member, IEEE*, Jin-Seob Kang, *Member, IEEE*, and Hosung Choo, *Senior Member, IEEE*

***Abstract*—The conventional Wheeler cap method usually produces accurate radiation efficiency of small antennas when the antennas under test (AUTs) operate as a simple series or a parallel RLC resonance circuit. However, this method often gives unreliable radiation efficiency if the AUT has a complicated operating principle such as circular polarization (CP), multiple resonances, or broad-band properties. In this paper, we propose an improved Wheeler cap method based on the equivalent high-order circuit model including transformers to provide accurate radiation efficiency, although the AUT does not operate as a simple resonance circuit. For building equivalent high-order circuit models, a method for estimating the initial values of a genetic algorithm (GA) is also proposed, which effectively reduces the searching space and improves the convergence of the optimization. To verify the proposed method, we measure the radiation efficiency of a CP microstrip antenna, a UHF RFID tag antenna, and a triple-resonance microstrip antenna.**

***Index Terms*—Efficiency, equivalent circuit, heuristic optimization, small antennas, Wheeler cap.**

I. Introduction

As various wireless services such as CDMA, GSM, Wi-Fi, and WiMAX have been developed, demands for extremely small antennas that can be mounted on small and light devices, have been growing. However, as antennas become smaller, their radiation efficiency decreases rapidly. Furthermore, the lossy substrate can give additional decrement in their radiation efficiency. The resulting poor radiation efficiency is a primary factor contributing to the reduction of antenna gain, although the antenna matches well with the feeding parts. Thus, the estimation and the measurement of radiation efficiency are critical in the design of small antennas.

In 1959, Wheeler reported a theory about the radiansphere, which is a boundary of the far-field and near-field regions with a distance of $\lambda/(2\pi)$ from a small antenna. The inside field of the radiansphere is mainly involved in the loss power and stored energy, while the outside field is involved in the radiation power. Wheeler's theory is that the radiation power can be removed from the antenna without disturbing the loss power and stored energy when it is shielded by placing the conducting cap on the radiansphere [1]. In [2], it was found that the size, shape, and conductivity of the conducting cap are not critical; that was analytically proved by [3]. In the conventional Wheeler cap method, radiation efficiency is obtained by comparing the input resistances in free-space and in the cap, which is as follows:

$$\mathrm{Eff} = \frac{P_{\mathrm{rad}}}{P_{\mathrm{rad}} + P_{\mathrm{loss}}} = \frac{R_{\mathrm{rad}}}{R_{\mathrm{rad}} + R_{\mathrm{loss}}} = 1 - \frac{R_{\mathrm{cap}}}{R_{\mathrm{free-space}}} \tag{1}$$

where R_{cap} and $R_{\mathrm{free-space}}$ are the input resistances with and without the conducting cap, respectively. This assumes that the AUT operates as a simple series RLC circuit in the operating frequency range. It is also known that the comparison of the input conductances is more appropriate than that of the input resistances when the AUT operates as a parallel RLC circuit [4], [5].

However, the conventional Wheeler cap method may not be applicable for complicatedly operating antennas since their loss mechanisms cannot be modeled as either a series or a parallel RLC circuit [4]. Several methods have been proposed to solve this problem. In order to consider the AUT as a series (or parallel) RLC circuit, the rotating reflection coefficient method forces the reactance at the resonance frequency to be zero using the port extension (i.e., shifting the reference plane) [6]. This method can enhance accuracy; but it is valid only near the resonance frequency. UWB Wheeler cap method can measure the radiation efficiency in a wide frequency region by using a large conducting cap [7]–[9]. This method assumes that the radiating power of the AUT can be represented as an infinite sum of radiation efficiency and S_{11} when all the radiation energy is reflected by the cap without any loss. However, various cavity modes occurring due to the large conducting cap degrade measurement accuracy. A method using a sliding cavity was proposed to solve the problem of accuracy degradation from the cavity resonances in a wide frequency range by varying the cap size [10], [11]. This method increases the measurement cost due to the movable cavities and multiple number of measurements (more than three measurements are needed). Detailed results for the above methods have been summarized in [12].

In this paper, to apply the Wheeler cap method to complicatedly operating antennas in a wide frequency range, an equivalent high-order circuit method is introduced and the radiation efficiency is calculated from that circuit. The proposed method shows superior results in wide frequency ranges while the conventional Wheeler cap method produces unreliable results. In addition, the high-order circuit including transformers is proposed as a general circuit model that can be used to easily build an equivalent circuit using a few lumped elements. Subsequently, a simple scheme used to guess the lumped elements in the equivalent circuit using a heuristic optimization algorithm such as a ge-

Manuscript received January 27, 2013; revised August 14, 2013; accepted October 02, 2013. Date of publication October 24, 2013; date of current version December 31, 2013. This work was supported by the Korea Research Institute of Standards and Science under the project Development of Technologies for Next-generation Electromagnetic Wave Measurement Standard Grant 13011011.

C. Cho and J. Kang are with the Center for Electromagnetic Wave, Korea Research Institute of Standards and Science, Daejeon 305-340, Korea.

H. Choo is with the School of Electronic and Electrical Engineering, Hongik University, Seoul 121-791, Korea (e-mail: hschoo@hongik.ac.kr).

Digital Object Identifier 10.1109/TAP.2013.2287277

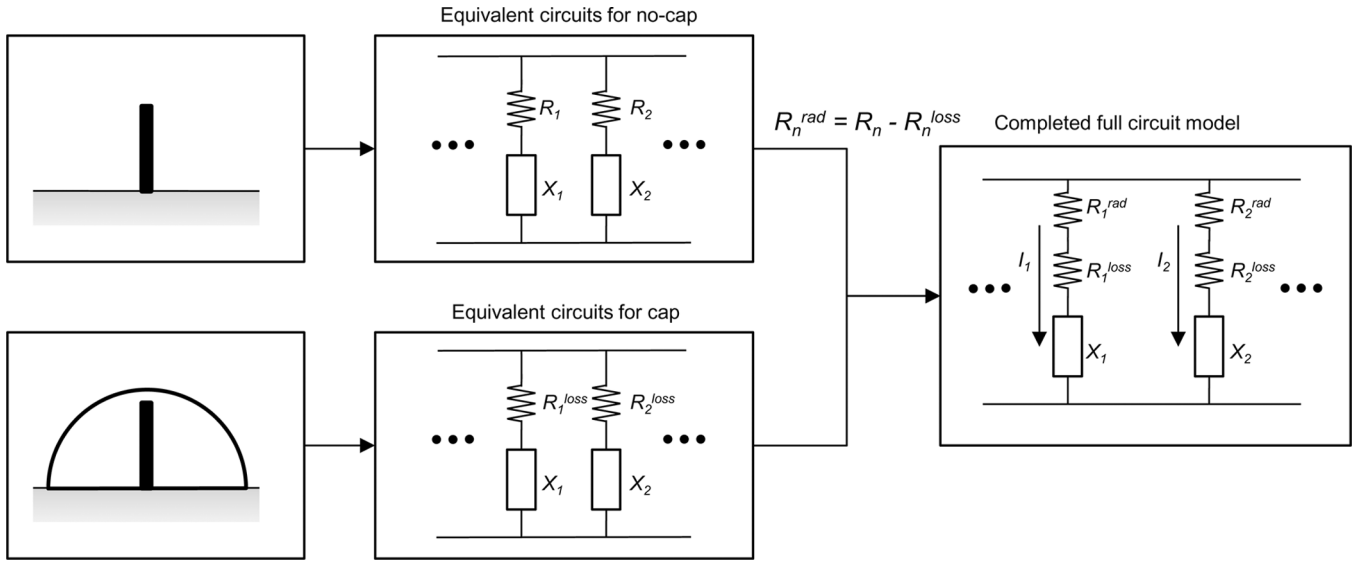

Fig. 1. Concept of the improved Wheeler cap method.

netic algorithm (GA) is proposed. Finally, the proposed method is confirmed by measuring the radiation efficiency of complicatedly operating antennas such as a CP microstrip antenna, a UHF RFID tag antenna, and a triple-resonance microstrip antenna. This paper is organized as follows. In Section II, we explain the concept of the proposed improved Wheeler cap method and the verification results. Section III describes how the lumped element values in the equivalent circuit are estimated using the heuristic optimization algorithm. Section IV presents the conclusions gathered from this research.

II. Description of the Proposed Method

A. Concept of the Improved Wheeler Cap Method

When an AUT has a complicated operating principle, it usually has multiple radiating modes. These modes are tightly linked, and the input resistance on those modes is highly dependent on the loss mechanism of the AUT. In such cases, the conventional Wheeler cap method often gives unreliable results since the radiation efficiency is obtained by simply comparing the variation of the input resistances without considering the radiating modes.

We employ a high-order circuit model to properly represent the characteristics of each radiating mode and to perform a more accurate radiation efficiency measurement. If the equivalent circuit describes the AUT's loss mechanism well, it can represent the input impedances of AUT in free-space as well as with the conducting cap by only changing the resistors' values. The full circuit modeling can be completed by finding both the loss resistors and the radiation resistors. Then, the radiation efficiency can be obtained

$$\mathrm{Eff} = \frac{P_{\mathrm{rad}}}{P_{\mathrm{rad}} + P_{\mathrm{loss}}} = \sum_{\mathrm{i}=1}^{\mathrm{N}} \frac{|I_i|^2 \times R_i^{\mathrm{rad}}}{|I_i|^2 \left(R_i^{\mathrm{rad}} + R_i^{\mathrm{loss}}\right)} \qquad (2)$$

where I_i is the current in the ith mesh, N is the number of meshes, and R_i^{rad} and R_i^{loss} are the radiation and loss resistors used in the circuit model, respectively. Fig. 1 shows the proposed concept graphically. The proposed method has several features as follows:

- It does not require one to know whether the loss mechanism of the AUT operates as a series or a parallel circuit.
- It can be applied in a wide frequency range in which the cavity resonance does not occur.
- It does not require a special conducting cap such as a moving cavity.
- Radiation efficiency can be obtained from only two impedance measurements as with the conventional Wheeler cap method.
- Accuracy of radiation efficiency is dependent upon the equivalent circuit for the AUT.

Thus, building an equivalent circuit to represent the loss mechanism of the AUT is critical in the proposed method. The radiation efficiency measurement of a probe-fed patch antenna using a cascade parallel circuit model was explained in [13].

B. High-Order Circuit Including Transformers

It is well known that the complex impedance of an antenna can be represented as a rational function, and that an equivalent circuit model can be constructed from that function using network theory [14], [15]. Recently, to find accurate coefficients of the rational function, several methods such as Cauchy and Vector fitting have been suggested [16], [17].

We use the high-order transformer circuit, as shown in Fig. 2, to simply build the equivalent circuit model. The proposed transformer circuit model consists of one series RLC circuit for the input terminal, shown on the left side of Fig. 2, and several series RLC circuits that are connected with the input circuit by mutual coupling M. The impedance of each RLC circuit is defined as (3), and the total impedance of the equivalent circuit is defined as (4)

$$Z_i = R_i + j\omega L_i + \frac{1}{j\omega C_i}, \quad (i = 1, 2, \ldots, N) \qquad (3)$$

$$Z_{\mathrm{in}} = Z_1 + \frac{\omega^2 M_2^2}{Z_2} + \frac{\omega^2 M_3^2}{Z_3} + \cdots + \frac{\omega^2 M_N^2}{Z_N}. \qquad (4)$$

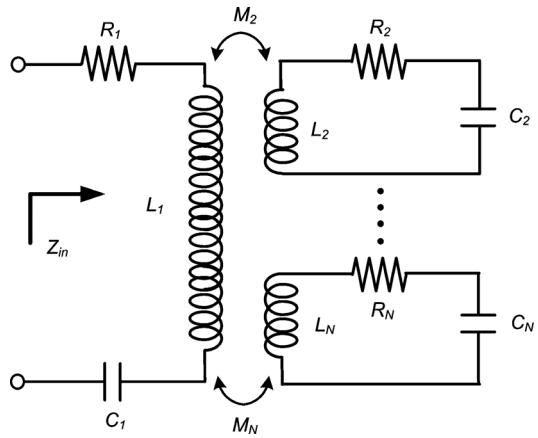

Fig. 2. The high-order transformer circuit.

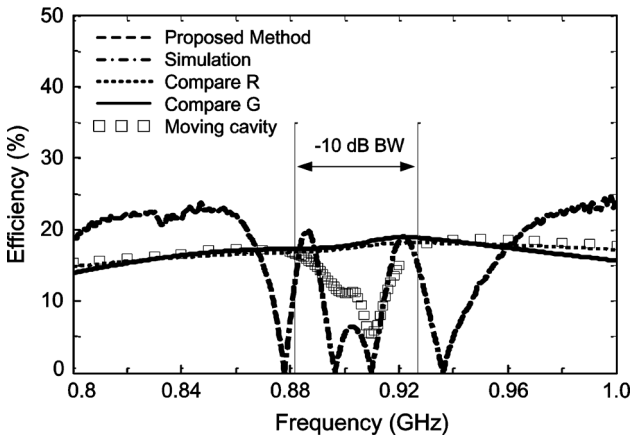

Fig. 3. Radiation efficiency of a CP microstrip antenna.

The impedance Z_1 on the input terminal describes the gradual slope of the impedance curve, and the mutually connected circuits $(Z_2 \cdots Z_N)$ describe fluctuations on the impedance curve at their resonance frequencies. The strength of the fluctuation is determined by the amount of the mutual coupling M, and the number of required transformers is the same as that of the resonances in the AUT. Thus, if the AUT has clean multiple resonances, the proposed high-order transformer circuit can be more easily and intuitively constructed with a small number of lumped RLC elements than the rational function method. An automated method for estimating lumped element values using a heuristic optimization algorithm (such as a GA) will be explained in Section III.

C. Measurement Results

The conventional Wheeler cap method assumes that an AUT operates as a simple RLC resonance circuit in the operating frequency range. However, that method often shows unreliable radiation efficiency when the AUT has a complicated operating principle. Fig. 3 shows the measured results of a CP microstrip antenna using the conventional Wheeler cap method. The antenna has a patch size of 78 mm $\times$ 81 mm and uses an FR-4 $(\varepsilon_{\rm r} = 4.25, \tan\delta = 0.002)$ substrate with a thickness of 1.6 mm. A probe feed is located on the diagonal line of the patch with a distance of 0.25 times the patch width from the center.

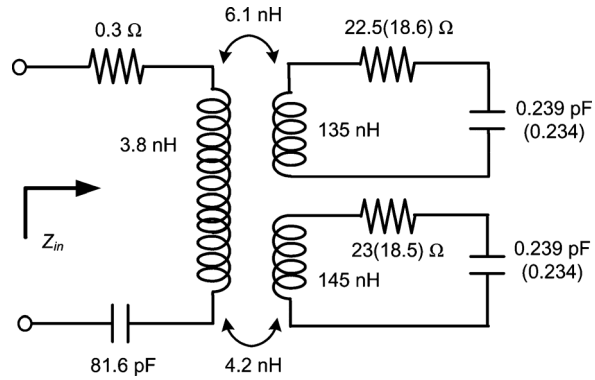

Fig. 4. The equivalent high-order transformer circuit model for a CP microstrip antenna.

The bandwidth ($|S_{11}| < -10$ dB) ranges from 882 MHz to 926 MHz with dual resonances and has an axial ratio of about 3 dB in the operating frequency range. The rectangular cap of 10 cm $\times$ 10 cm $\times$ 5 cm is used to prohibit the generation of the cavity mode in the measurement. The dashed and dashed-dotted lines represent the radiation efficiency using the conventional Wheeler cap method (comparing R or G), and the dotted line represents the simulation results obtained from comparing the gain and directivity using HFSS [18]. The conventional Wheeler cap method, both comparing resistance and conductance, does not match with the simulation results (comparing R is an RMS difference of 10.48% and comparing G is an RMS difference of 15.41%) in the operating frequency range. When the loss mechanism of the AUT is drastically changed from a series circuit to a parallel circuit or vice versa (for example, at 880 MHz and 940 MHz in Fig. 3), the conventional Wheeler cap method shows a null value in the radiation efficiency measurement since the loss mechanism cannot be represented as a simple series or a parallel RLC circuit. The moving cavity method (represented with square marks on Fig. 3) also shows similar phenomena in these frequency bands [10], [11], and it means that this null value cannot be corrected by removing cavity resonances.

The proposed equivalent circuit model of the CP antenna with lumped RLC values is shown in Fig. 4. The parenthetical values are those that resulted when the antenna was shielded by the cap, while the non-parenthetical values are the element values in free-space. Antenna resistance decreases after the cap is installed, because the shielding of the antenna prevents far-field radiation, which reduces the resistance. Therefore, the radiation efficiency can be determined by the decreased ratio of the resistance. Small changes in capacitances occur due to the parasitic capacitance between the cap and each part of the antenna. The measured and circuit model impedances in free-space are shown in Fig. 5(a), and the results with the cap are shown in Fig. 5(b). Input impedances of the circuit both in the free-space and in the cap match well with the measurement results. The antenna efficiency is calculated using (2) from the built circuit, and it is plotted in Fig. 3 with a solid line. The efficiencies of the circuit model and the simulation show good agreement with an RMS difference of 0.65%, while the conventional Wheeler cap method provides RMS differences of 10.48% (comparing R), and 15.41% (comparing G), respectively.

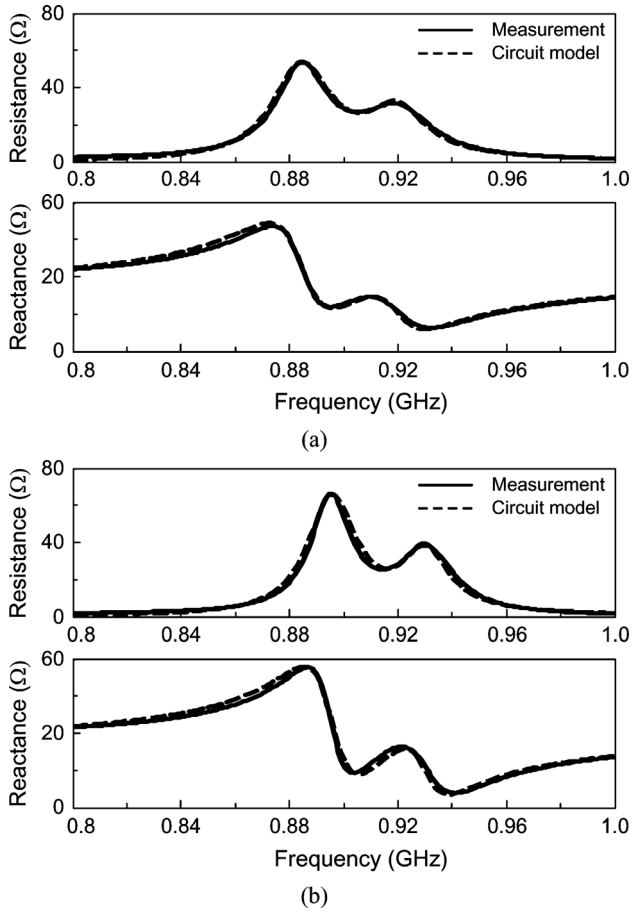

Fig. 5. Input impedance using the high-order transformer circuit model and measurement for CP microstrip antenna (a) in free-space and (b) with the cap.

III. Fitting the Circuit Parameters Using GA

A. Setting the Initial Values

Heuristic optimization methods such as a GA and a PSO can quickly find the optimum solution [19], [20]. However, these methods may not produce good results when working in a large searching space with initial values that are far away from the optimum solution. Thus, we propose a method that can determine the proper initial values for a more efficient optimization process and for reducing the searching space.

In the previous section, we mentioned that the RLC values of the input terminal Z_1 describe the gradual slope on the total impedance with respect to frequency, and the other mutually connected circuits $(Z_2, \ldots, Z_{\mathrm{N}})$ describe the fluctuated impedance on each resonance frequency. Thus, the circuit parameters may be given by

$$R_1 = (R_{\mathrm{meas.}}(f_{\mathrm{start}}) + R_{\mathrm{meas.}}(f_{\mathrm{end}}))/2 \tag{5}$$

$$j\omega(f_{\mathrm{start}})L_1 + \frac{1}{j\omega(f_{\mathrm{start}})C_1} = X_{\mathrm{meas.}}(f_{\mathrm{start}}) \tag{6}$$

$$j\omega(f_{\mathrm{end}})L_1 + \frac{1}{j\omega(f_{\mathrm{end}})C_1} = X_{\mathrm{meas.}}(f_{\mathrm{end}}) \tag{7}$$

where f_{start} and f_{end} are the start and end frequencies in the measured frequency range, respectively. Small impedance fluctuations at f_{start} and f_{end} are assumed to closely represent the gradual slope of the impedance curve. Subsequently, L_1 and C_1 can be found by solving (6) and (7), and R_1 is set to averaged resistances at f_{start} and f_{end}. Next, the lumped element values of the mutually connected series circuits are determined using (8)–(10)

$$M_i = \sqrt{\frac{\left(R_{\mathrm{meas.}}\left(f_i^{\mathrm{peak}}\right) - R_1\right) \times R_i}{\left(2\pi f_i^{\mathrm{peak}}\right)^2}} \tag{8}$$

$$L_i = \frac{M_i^2\left(2\pi f_i^{\mathrm{peak}}\right)}{\left(X_{\mathrm{meas.}}\left(f_i^{\mathrm{peak}}\right) - X_1\left(f_i^{\mathrm{peak}}\right)\right)} \tag{9}$$

$$C_i = \frac{1}{\left(2\pi f_i^{\mathrm{peak}}\right)^2 L_i}, \quad (i = 2, 3, \ldots, N). \tag{10}$$

In (8)–(10), f_i^{peak} is the frequency where the fluctuation of the measured input resistance peaks. X_1 is the imaginary value of input terminal circuit (Z_1) using L_1, C_1, and R_1 from (5)–(7). Then, L_i, C_i, and R_i are lumped values of the mutually connected ith RLC circuit, and M_i is the strength of mutual coupling between the input terminal and the connected circuits. In our case, we set R_i to 50 Ω, which is usually used as the characteristic impedance in RF systems.

Fig. 6 shows the impedance at each step of the initial value-setting procedure. Fig. 6(a) shows each resistance of the mutually connected RLC circuits on the input terminal after determining the mutual coefficients using (5)–(8). At each resonance frequency, the mutual coupling coefficients are determined; the peaks of $R_i (i \geq 2)$ on the input terminal are equal to the measured data. Fig. 6(b) also represents each resistance after determining L_i using (9). Each resistance slowly changes compared with the results in Fig. 6(a), since the quality factors of each circuit are decreased by setting L_{i}. Fig. 6(c) describes each reactance of the mutually connected circuit after setting C_i to describe the fluctuation at each resonance frequency. Fig. 6(d) shows the total input impedance of the high-order transformer circuit, which includes the input terminal impedance using (5)–(10). The total input impedance is quite similar to the measured data, and it shows that the proposed procedure could effectively reduce the searching space.

We then apply a GA to find optimal values of lumped elements in the circuit model, and the flow diagram of the proposed method using the GA is shown in Fig. 7. The searching space of the GA is determined from the initial values using (5)–(10), and the lumped RLC values are obtained within the searching space. Total impedance of the circuit (Z_{in}) is calculated and compared with the measured data, and that circuit is evaluated by the cost function as follows:

$$\mathrm{cost} = \left(\sum_{i=1}^{k} Z_{\mathrm{meas.}}(f_i) - Z_{\mathrm{in}}(f_i)\right)/k \tag{11}$$

where k is the measured frequency points. The cost function is defined as the difference between the measured $(Z_{\mathrm{meas.}})$ and circuit modeled impedances (Z_{in}). As the cost value decreases, the resulting RLC values approach the optimum

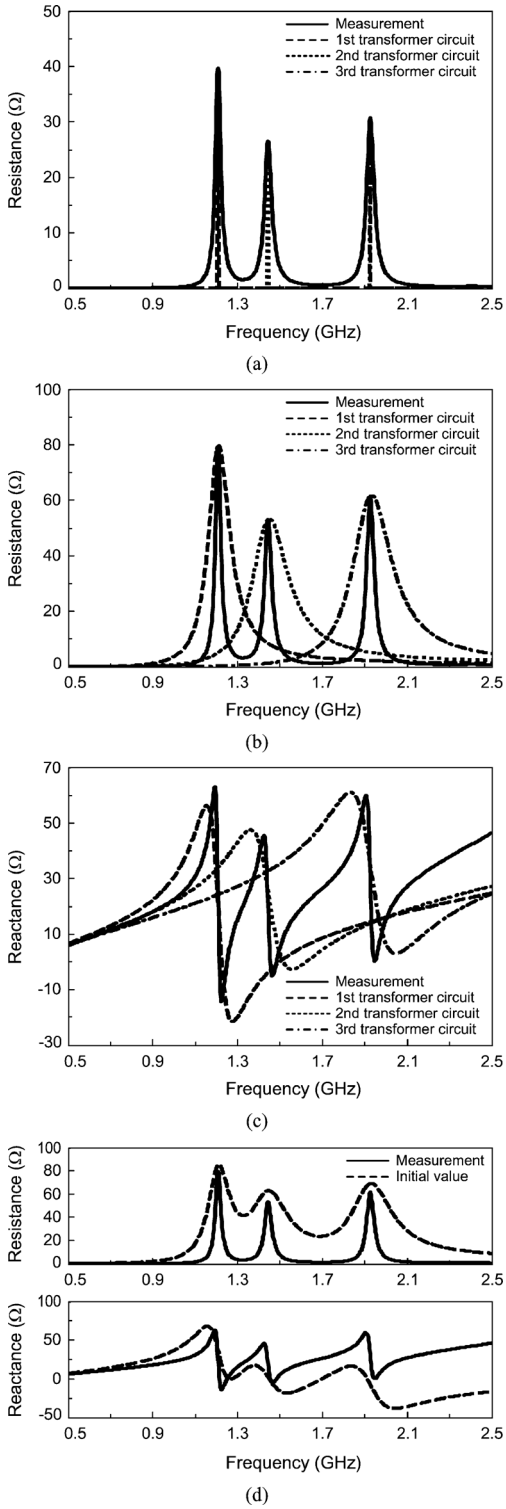

Fig. 6. The impedance for the procedure of determining the initial value. (a) Resistance of each transformer after determining initial M. (b) Resistance of each transformer after initial inductance. (c) Reactance of each transformer after determining initial capacitances. (d) Total input impedance after determining initial values.

solution. During the iteration of this procedure, the transformer circuit model could be fitted more accurately to the measured impedance in free-space. The same procedure is applied to obtain the lumped RLC values for the measured impedance in the cap. Finally, the antenna radiation efficiency can be

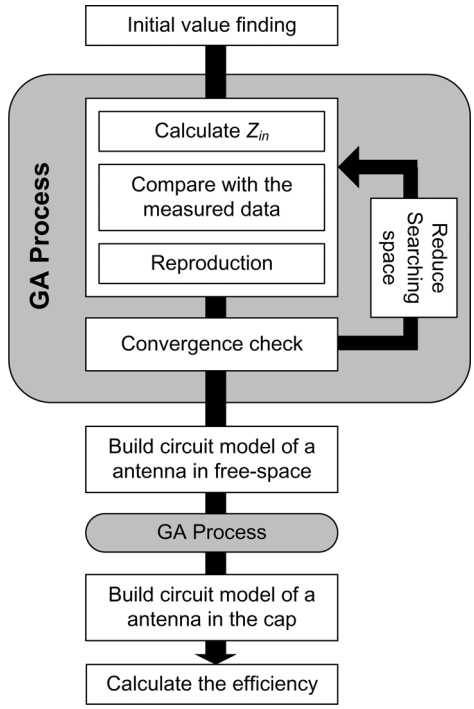

Fig. 7. The flow diagram of the proposed modified Wheeler cap method using a GA.

obtained from the power dissipation ratio of each resistance after separating the radiating and loss resistances using the proposed Wheeler cap method. Thus, the proposed method based on GA using initial value setting procedure should meet two conditions; First, AUT should have clean resonances which can be represented by the high order transformer circuit model. Second, the measurement should be performed below the cavity resonance frequency since it cannot be easily represented using the equivalent circuit model.

B. Measurement Results Using GA

We finally apply the GA process in conjunction with the initial value estimating method to the radiation efficiency measurement for an RFID tag antenna. The passive tag antenna ($kr = 0.43$) in [21] is used, and that antenna operates at 914 MHz. The same rectangular cap of 10 cm × 10 cm × 5 cm is also applied. Generally, inaccurate measurement results are expected with the conventional Wheeler cap method, since the passive tag antennas are designed for matching to the tag chip's conjugate impedance instead of a 50 Ω characteristic impedance. In the high-order circuit, one transformer is introduced since the measured data have one large fluctuation in the input impedance. The optimized input impedance using the GA with the high-order transformer circuit is shown in Fig. 8(a). The impedances from measurement and the equivalent circuit are represented by the solid and dashed lines, and they show good agreement with an RMS difference of 2.3 Ω for the input resistance and 30.5 Ω for the input reactance, respectively. The lumped RLC values of the circuit are summarized in Table I. Both the impedance from the measurement and the high-order circuit for the shielded tag antenna with the cap are represented in Fig. 8(b). The lumped

TABLE I
THE LUMPED RLC VALUES OF THE OPTIMIZED CIRCUIT MODEL (USING ONE TRANSFORMER) FOR THE RFID TAG ANTENNA

	R_1 (Ω)	R_2 (Ω)	L_1 (H)	L_2 (H)	C_1 (F)	C_2 (F)	M_2 (H)
Free- space	0.7932	49.9981	4.09337E-08	1.12585E-06	1.5638E-12	2.7962E-14	1.7650E-08
In the cap	0.6292	25.8066	4.09337E-08	1.12585E-06	1.5638E-12	2.8150E-14	1.7650E-08

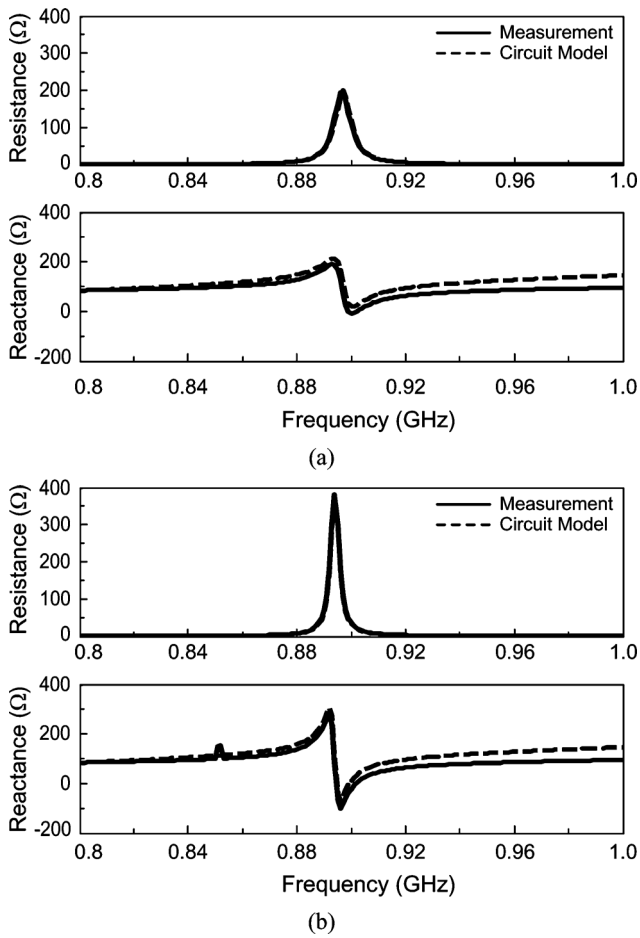

Fig. 8. Input impedance using the high-order transformer circuit model and measurement for RFID tag antenna (a) in free-space and (b) with the cap.

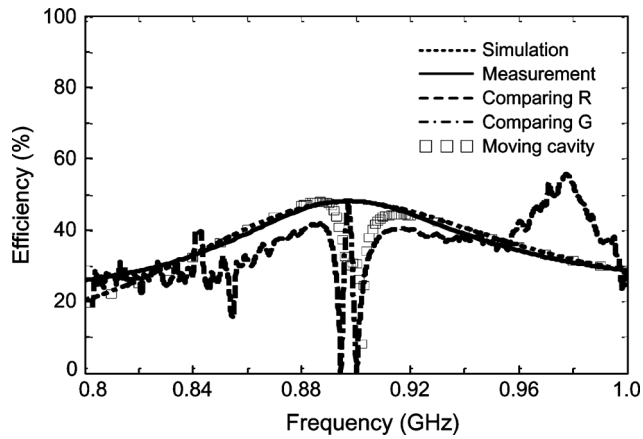

Fig. 9. Efficiency of RFID tag antenna.

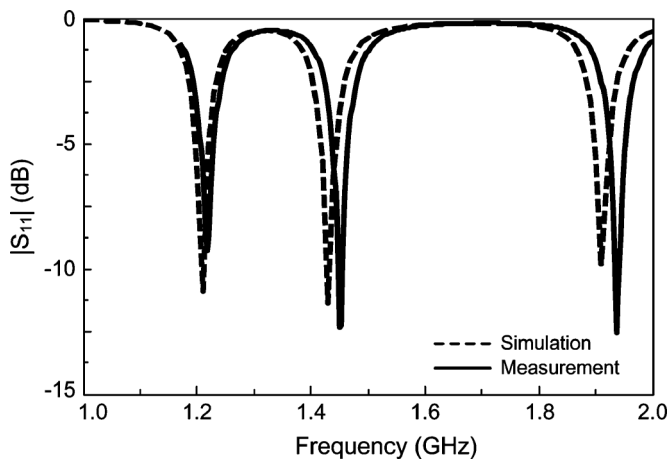

Fig. 10. S_{11} of the triple-resonance microstrip antenna.

RLC values in the cap are also summarized in Table I. As expected, the values of the inductor and mutual coupling coefficient are not changed, although the AUT is shielded by the conducting cap. However, the values of the capacitor are slightly changed due to the parasitic capacitance between the AUT and the cap.

Next, we separate each resistance in the free-space circuit model into radiating and loss resistances using the shielded circuit model. The antenna's efficiency is calculated based on the power consumption ratio of each separated resistance, and the result is plotted in Fig. 9 with the solid line. The simulated radiation efficiency is determined using the EM simulator; results using the conventional Wheeler cap and moving cavity methods are also plotted in the same figure as dotted, dashed (comparing R), dashed-dotted line (comparing G), and square marks (moving cavity). The results clearly show that the proposed improved Wheeler cap method with the GA process shows more accurate result with an RMS difference of 1.71% compared to the conventional Wheeler cap and moving cavity methods with RMS differences 12.83% (comparing R), 37.59% (comparing G), and 2.95% (moving cavity), respectively.

Finally, we apply the improved Wheeler cap method using the GA for the triple-resonance microstrip antenna. The antenna has a patch size of 60 mm × 50 mm, and it is printed on a FR-4 ($\varepsilon_r = 4.25, \tan\delta = 0.002$) substrate with thickness of 1.6 mm. A probe feed is located at the same position as the CP patch in Section II, and the same cap also used. The measured S_{11} of the microstrip antenna is shown in Fig. 10, and it shows triple resonances at approximately 1.2 GHz, 1.45 GHz, and 1.9 GHz. The three transformers are employed to model the triple resonances of the antenna, and the optimized RLC values in free-space and in the cap are listed in Table II. Fig. 11(a)

TABLE II
THE LUMPED RLC VALUES OF THE OPTIMIZED CIRCUIT MODEL (USING THREE TRANSFORMERS) FOR THE TRIPLE RESONANCES MICROSTRIP ANTENNA

Free-space	R_1 (Ω)	R_2 (Ω)	R_3 (Ω)	R_4 (Ω)	L_1 (H)	L_2 (H)	L_3 (H)	L_4 (H)
	0.3472	45.3578	24.0506	12.6761	3.5276E-09	2.6898E-07	9.8316E-08	4.8882E-08
	C_1 (F)	C_2 (F)	C_3 (F)	C_4 (F)	M_2 (H)	M_3 (H)	M_4 (H)	
	2.3086E-11	6.4586E-14	1.2382E-13	1.3984E-13	8.1591E-09	3.9403E-09	2.2807E-09	
In the cap	R_1 (Ω)	R_2 (Ω)	R_3 (Ω)	R_4 (Ω)	L_1 (H)	L_2 (H)	L_3 (H)	L_4 (H)
	0.3471	38.2467	16.9486	11.191	3.5276E-09	2.6898E-07	9.8316E-08	4.8882E-08
	C_1 (F)	C_2 (F)	C_3 (F)	C_4 (F)	M_2 (H)	M_3 (H)	M_4 (H)	
	2.3086E-122	6.4055E-14	1.2254E-13	1.3948E-13	8.1591E-09	3.9403E-09	2.2807E-09	

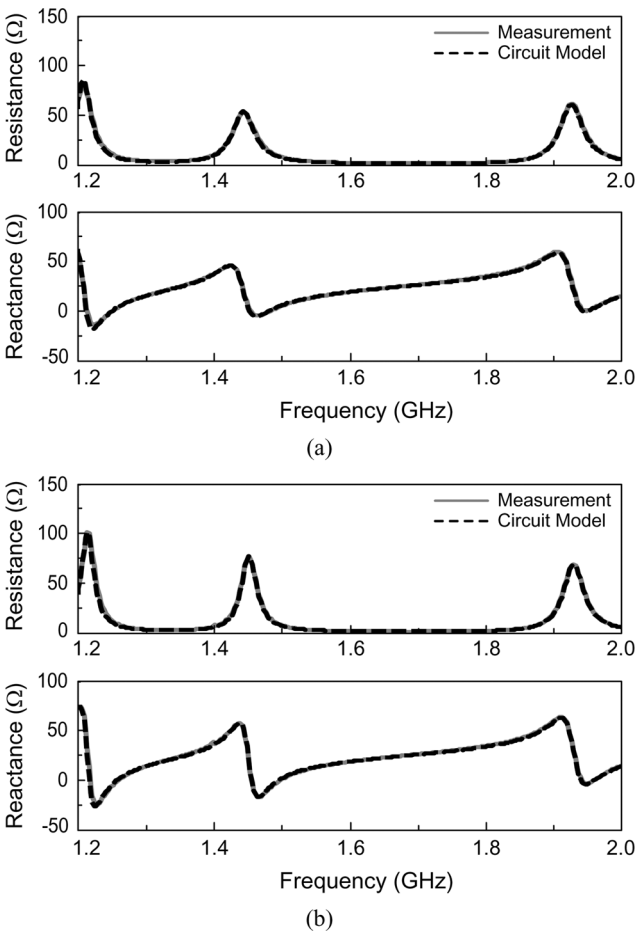

Fig. 11. Input impedance using the high-order transformer circuit model and measurement for the triple resonance microstrip antenna (a) in free-space and (b) with the cap.

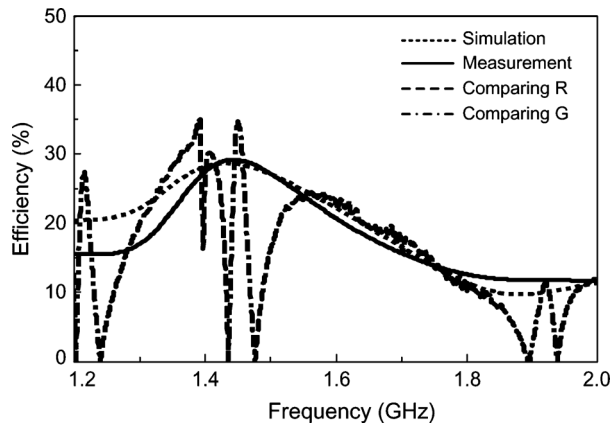

Fig. 12. Efficiency of the triple-resonance microstrip antenna.

shows the measured input impedance (solid line) and the computed one using the GA (dashed line) when the antenna is in free-space. The results of the input impedance with the cap are also shown in Fig. 11(b). Both the impedances in free-space and with the cap closely resemble the measurement results. The radiation efficiency using the proposed method and the conventional Wheeler cap method are shown in Fig. 12. The results using the conventional Wheeler cap method are represented by a dashed (comparing R) and a dashed-dotted line (comparing G). The solid line represents the radiation efficiency of the proposed method using the GA, and the dotted line shows the simulation result using the EM simulator [16]. The radiation efficiency of the improved Wheeler cap method using the GA shows an RMS difference of 2.45% with that of the simulation while the conventional Wheeler cap exhibits RMS differences of 11.28% (comparing R), and 19.76% (comparing G), respectively.

We investigate how the accuracy of efficiency measurement depends on the accuracy of the equivalent circuit. The difference between the circuit impedance and the measurement is compared to the error of the efficiency measurement by calculating a correlation value. A high correlation of 0.9 is observed for the example of the RFID tag antenna in Fig. 9. This indicates that the accuracy of the proposed method is dependent on the equivalent circuit for the AUT.

We also perform a type-A uncertainty evaluation for the proposed method by conducting 20-times repeated measurements. The result shows an uncertainty value of 2.8% with 95% confidence level, which is slightly higher than the value presented in [4]. More detailed uncertainty can be achieved by performing a type-B uncertainty evaluation, which separately analyzes each uncertainty factor expected in the measurement procedure [23].

IV. Conclusion

In this paper, we proposed an improved Wheeler cap method based on a high-order transformer circuit for obtaining accurate radiation efficiency of small antennas. To confirm the proposed method, we apply the method to a CP microstrip antenna. The resulting radiation efficiency showed good agreement with the simulated one in a wide frequency range (within RMS difference of 2.45%), while the conventional Wheeler cap method produces unreliable results (RMS difference is 10.48% to 37.59%), especially for frequencies where the loss mechanism drastically changed from a series circuit to a parallel circuit or vice versa. Since the accuracy of the proposed method is dependent upon that of the built circuit model, the circuit values were obtained automatically using a heuristic optimization algorithm. To effectively reduce the searching space in the optimization, a scheme for determining an initial value was also provided. Finally, the radiation efficiencies of complicatedly operating antennas such as an UHF RFID tag and a patch antenna with triple resonances were measured and compared with that using the conventional Wheeler cap method. The results in all cases clearly showed that the proposed method can achieve better results than the conventional Wheeler cap method.

References

[1] H. A. Wheeler, "The radiansphere around a small antenna," *Proc. IRE*, pp. 1325–1331, Aug. 1959.

[2] E. H. Newman, P. Bohley, and C. H. Walter, "Two methods for the measurement of antenna efficiency," *IEEE Trans. Antennas Propag.*, vol. 23, pp. 457–461, July 1975.

[3] G. S. Smith, "An analysis of the Wheeler method for measuring the radiation efficiency of antennas," *IEEE Trans. Antennas Propag.*, vol. 25, pp. 552–556, Jul. 1977.

[4] D. M. Pozar and B. Kaufman, "Comparison of three methods for the measurement of printed antenna efficiency," *IEEE Trans. Antennas Propag.*, vol. 36, pp. 136–139, Jan. 1988.

[5] H. Choo, R. Rogers, and H. Ling, "On the Wheeler cap measurement of the efficiency of microstrip antennas," *IEEE Trans. Antennas Propag.*, vol. 53, pp. 2328–2332, Jul. 2005.

[6] W. E. McKinzie, "A modified Wheeler cap method for measuring antenna efficiency," in *IEEE Antennas Propagat. Soc. Int. Symp.*, July 1997, vol. 1, pp. 542–545.

[7] H. G. Schants, "Radiation efficiency of UWB antennas," in *IEEE Conference on. Ultra Wideband Systems and Technologies*, May 2002, pp. 351–355.

[8] M. C. Huynh, "Wideband Compact Antenna for Wireless Communication Applications," Ph.D. dissertation, Virginia Pol. Inst. State Univ., Blacksburg, VA, USA, 2004.

[9] Y. Huang, Y. Lu, S. Boyes, and T.-H. Loh, "Source-stirred chamber/cap method for antenna radiation efficiency measurements," in *Proc. Eur. Conf. Antennas Propag. (EuCAP)*, Rome, Italy, Apr. 2011, pp. 164–168.

[10] R. H. Johnston and J. G. McRory, "An improved small antenna radiation-efficiency measurement method," *IEEE Antennas Propag. Mag.*, vol. 50, pp. 40–48, Oct. 1998.

[11] N. Ishii and M. Miyakawa, "Analysis on the dips of the radiation efficiency in the reflection method using the transmission line model," in *Proc, IEEE Int. Workshop Antenna Technology Small Antennas Novel Metamaterials*, Mar. 2006, pp. 313–316.

[12] P. Miskovsky, J. M. Gonzalez-Arbesu, and J. Romeu, "Antenna radiation efficiency measurement in an ultrawide frequency range," *IEEE Antennas Wireless Propag. Lett.*, vol. 8, pp. 72–74, 2009.

[13] C. Cho, I. Park, and H. Choo, "A modified Wheeler cap method for efficiency measurements of probe-fed patch antennas with multiple resonances," *IEEE Trans. Antennas Propag.*, vol. 58, pp. 3074–3078, Sep. 2010.

[14] Y. Kim and H. Ling, "Realisable rational function approximations for the equivalent circuit modelling of broadband antennas," *IET Microwave Antennas Propag.*, vol. 55, pp. 1046–1054, Oct. 2007.

[15] F. F. Kuo, *Network Analysis and Synthesis*. New York, NY, USA: Wiley, 1962.

[16] R. S. Adve, T. K. Sarkar, S. M. Rao, E. K. Miller, and D. R. Pflug, "Application of the Cauchy method for extrapolating/interpolating narrow-band system responses," *IEEE Trans. Microwave Theory Tech.*, vol. 45, pp. 837–845, May 1997.

[17] B. Gustavsen and A. Semlyen, "Rational approximation of frequency domain responses by vector fitting," *IEEE Trans. Power Delivery*, vol. 14, pp. 1052–1061, July 1999.

[18] Ansoft Corporation HFSS. [Online]. Available: http://www.ansoft.com/products/hf/hfss/

[19] R. L. Haupt, "An introduction to genetic algorithms for electromagnetics," *IEEE Antennas Propag. Mag.*, vol. 37, pp. 7–15, Apr. 1995.

[20] J. Robinson and Y. Rahmat-Samii, "Particle swarm optimization in electromagnetics," *IEEE Trans. Antennas Propag.*, vol. 52, pp. 397–407, Feb. 2004.

[21] C. Cho, H. Choo, and I. Park, "Design of UHF small passive tag antennas," in *IEEE Antennas Propagat. Soc. Int. Symp.*, July 2005, vol. 2B, pp. 349–352.

[22] [Online]. Available: http://www.zeland.com/ie3d.htmlZeland Software, IE3D MoM-based EM simulator

[23] Guide to the Expression of Uncertainty in Measurement ISO. Geneva, Switzerland, 1993.

Chihyun Cho (M'09) received the B.S., M.S., and Ph.D. degrees in electronic and electrical engineering from Hongik University, Seoul, Korea, in 2004, 2006, and 2009, respectively.

From 2009 to 2012, he was a senior research engineer with the Samsung Thales, where he worked on the development of various military communication systems. In 2012, he joined the Center for Electromagnetic Wave, Korea Research Institute of Standards and Science. His research interests include electromagnetic measurement standards, design and optimization of microwave devices and antennas.

Jin-Seob Kang (M'88) received the B.S. degree in electronic engineering from Hanyang University, Seoul, Korea, in 1987 and the M.S. and Ph.D. degrees in electrical engineering from the Korea Advanced Institute of Science and Technology, Daejeon, Korea, in 1989 and 1994, respectively.

In 1995, he was a Visiting Postdoctoral Research Associate with the Department of Electrical and Computer Engineering, University of Illinois at Urbana-Champaign, Urbana. From 1996 to 1997, he was an Assistant Professor with the School of Electrical and Electronics Engineering, Chungbuk National University, Cheongju, Korea. In 1998, he joined Korea Research Institute of Standards and Science, Daejeon. His research interests include electromagnetic measurement standards, impedance and antenna measurements, and electromagnetic wave scattering.

Hosung Choo (S'00–M'04–SM'11) was born in Seoul, Korea, in 1972. He received the B.S. degree in radio science and engineering from Hanyang University, Seoul, Korea, in 1998, and the M.S. and Ph.D. degrees in electrical and computer engineering from the University of Texas, Austin, TX, USA, in 2000 and 2003, respectively.

In September 2003, he joined the school of electronic and electrical engineering, Hongik University, Seoul, Korea, where he is currently an Associate Professor. His principal areas of research are the use of the optimization algorithm in developing antennas and microwave absorbers. His studies include the design of small antennas for wireless communications, reader and tag antennas for RFID, and on-glass and conformal antennas for vehicles and aircraft.